Mechanical loading and hyperosmolarity as a daily resetting cue for skeletal circadian clocks

Michal Dudek[1,2,3], Dharshika Pathiranage[1,2,3], Cátia F. Gonçalves[1,2,3], Craig Lawless[1,3], Dong Wang[4], Zhuojing Luo[4], Liu Yang[4], Judith Hoyland*[3,5], Qing-Jun Meng*[1,2,3]

[1]Wellcome Centre for Cell Matrix Research, Faculty of Biology, Medicine and Health, University of Manchester, Oxford Road, Manchester, UK

[2]Centre for Biological Timing, Faculty of Biology, Medicine and Health, University of Manchester, Oxford Road, Manchester, UK

[3]Division of Cell Matrix Biology and Regenerative Medicine, School of Biological Sciences, Faculty of Biology, Medicine and Health, University of Manchester, Manchester Academic Health Science Centre, Manchester, UK

[4]Institute of Orthopedic Surgery, Xijing Hospital, Fourth Military Medical University, Xi'an, China

[5]NIHR Manchester Biomedical Research Centre, Central Manchester Foundation Trust, Manchester Academic Health Science Centre, Manchester, United Kingdom

*Corresponding authors: Email: Qing-Jun.Meng@manchester.ac.uk; Judith.A.Hoyland@manchester.ac.uk

Abstract: In mammals, temporally coordinated daily rhythms of behaviour and physiology are generated by a multi-oscillatory circadian system, entrained through cyclic environmental cues (e.g. light). Presence of niche-dependent physiological time cues has been proposed, which would allow local tissues flexibility of adopting a different phase relationship if circumstances require. Up till now, such tissue-unique stimuli have remained elusive. Here we show that cycles of mechanical loading and osmotic stimuli within physiological range drive rhythmic expression of clock genes and reset clock phase and amplitude in cartilage and intervertebral disc tissues. Hyperosmolarity (and not hypo-osmolarity) resets clocks in young and ageing skeletal tissues through mTORC2-AKT-GSK3β pathway, leading to genome-wide induction of rhythmic genes. These results suggest diurnal patterns of mechanical loading and consequent daily surges in extracellular osmolarity as a bona fide tissue niche-specific time cue to maintain skeletal circadian rhythms in sync.

One-Sentence Summary: Circadian clocks in aneural skeletal tissues sense the passage of time through rhythmic patterns of loading and osmolarity.

Main Text:

The daily patterns of rhythmic environment on Earth, including light/darkness, temperature fluctuations, availability of food and presence of predation, have profound impacts on the physiology and behaviour of living organisms. To anticipate and cope with changing demands between day and night, most organisms have evolved an internal cell-intrinsic timing mechanism, the circadian clock. Close alignment of internal circadian rhythms with external environment (known as entrainment) is of paramount importance for health and survival (*1*). In mammals, the current model proposes that the central pacemaker Suprachiasmatic Nuclei (SCN) in the hypothalamus temporally coordinates and adjusts peripheral clocks in all major body organs (*2-4*). Light as a primary and potent clock entrainment factor resets the central clock which in turn signals directly (through neuronal connections) or indirectly through hormonal cues and body temperature to the rest of the body (*5-8*). However, one argument for the adaptive value of local tissue clocks (rather than simply a top down control from the SCN) is that they allow flexibility - peripheral clocks can adopt a different phase relationship with one another (and with the SCN) if circumstances require. If this argument is true, we would expect local clocks to be synchronised to the most physiologically relevant stimuli. One piece of evidence supporting this is the uncoupling of circadian clocks in the liver and other tissues from the SCN upon restricted feeding (*9-11*).

The mammalian skeletal system, especially the articular cartilage in joints and intervertebral disc (IVDs) in the spine, provides a unique model to resolve this question. Cartilage and IVDs are among the most highly loaded tissues in the body, experiencing a diurnal loading cycle associated with daily rest/activity patterns (*12*). They experience a prolonged period of compression of 2-3.5 MPa during the activity phase, followed by a period of low-load recovery during resting phase (down to 0.1 MPa). Cartilage and IVDs possess intrinsic circadian clocks that drive rhythmic expression of tissue specific genes and become dampened and out of phase in ageing mice. Genetic disruption of the cartilage and IVD clocks results in imbalance of anabolic and catabolic processes which subsequently leads to accelerated tissue ageing and degeneration (*13-17*). The aneural and avascular nature of articular cartilage and IVDs makes them less amenable to conventional systemic time cues conveyed through nerves or hormones (*12*). Therefore, it remains unknown how these skeletal clocks are entrained under physiological conditions. Indeed, we observed no difference in the potency of mouse serum collected during the day vs. night in their ability to synchronise these tissue clocks (Fig. S1). As such, blood-

borne serum factors are unlikely to be an effective clock resetting cue for these tissues (*18*). Given the diurnal loading patterns they experience, a priori should expect these peripheral skeletal clocks to be synchronised by some aspects of mechanical loading. However, up till now, this has not been shown. Therefore, we analysed the role of mechanical loading in resetting skeletal circadian clocks and addressed underlying mechanisms.

Mechanical loading resets the circadian clocks in femoral head cartilage and IVD

To test the role of mechanical loading, we used an *ex vivo* tissue explant culture model utilising the PER2::Luc reporter mouse which allows real-time monitoring of the endogenous clock protein PER2 using Lumicycle (*14, 15,19*). We found that a short loading regime (1 hour of 1 Hz, 0.5 MPa compression) resulted in robust amplitude increase of the circadian rhythm in cartilage which was maintained for at least three more days (Fig. 1A). To delineate the best response window within the 24 hour cycle, we applied the same compression protocol at 4 time points 6 hours apart. Only compression applied at the peak of PER2::Luc resulted in a significant increase of circadian amplitude ($p<0.001$, Fig. 1B,C), with minimal phase shift ($p>0.05$, Fig. 1D). Compression at other phases resulted in significant phase delay or advance (Fig. 1D). Compression applied at the trough disrupted circadian rhythm, highlighting the importance of the circadian phase in modulating the clock response to loading (Fig.1D). The phase shift of the cartilage circadian rhythm was dependent on the magnitude of the force of compression (Fig. 1E).

The same loading protocol altered the circadian PER2::Luc rhythm in IVD tissue in a similar manner (Fig.1F and Fig.S2). Although, the amplitude enhancing effect was not as pronounced as in cartilage, which may be partly due to the complex nature of the IVD tissue structure (with the nucleus pulposus core ensheathed by tightly organised annulus fibrosus rings and cartilage end plate). Next, we tested whether rhythmic loading patterns can entrain circadian rhythms of endogenous clock genes in IVD cells. To this end, rat IVD NP cells were subjected to oppositely phased mechanical loading cycles of 12-hour loading at 0.5 MPa /12-hour unloading. qPCR showed that the expression of clock genes *Bmal1* and *Cry1* were driven ~180 degrees out of phase (Fig. 1G), further supporting rhythmic loading as an endogenous clock resetting cue for cells in the skeletal system.

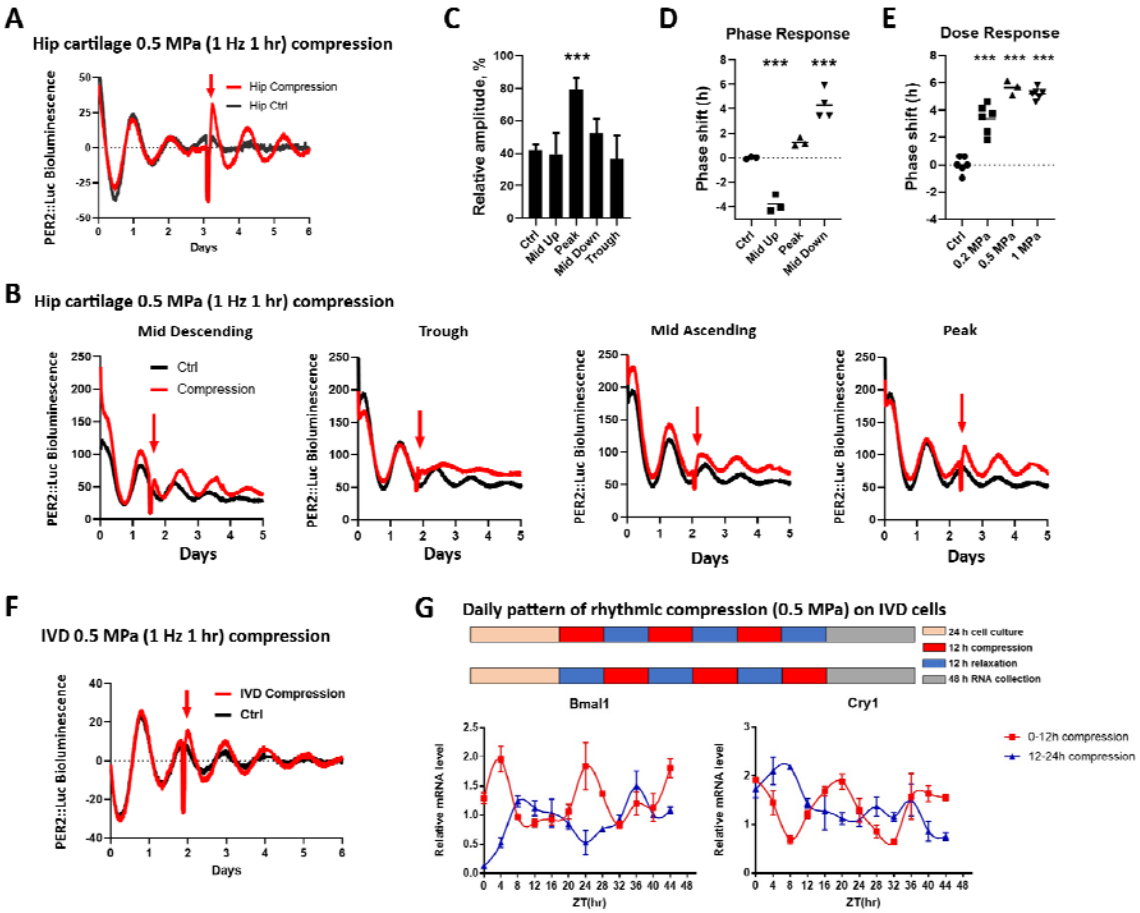

Figure 1. Mechanical loading resets the circadian clock in cartilage and IVDs in a phase and dose dependent manner. (**A**) Bioluminescence recordings of femoral head cartilage explants from PER2::Luc reporter mice. Red arrow indicates time of compression (0.5 MPa, 1 Hz, 1 hr). Each trace represents the mean of 3 explants. (**B**) Recordings of PER2::Luc cartilage explants subjected to mechanical loading (red arrow) at 6 hr intervals, starting at mid-descending phase. Each trace is the mean of 4 explants. (**C**) Quantification of the PER2::Luc amplitude change in **B**, expressed as % of the amplitude of the peak before loading. One-way ANOVA. ***p<0.001 vs. control. (**D**) Quantification of phase shifts in **B**. ***p<0.001 vs. control. (**E**) Quantification of phase shifts in cartilage exposed to increasing magnitude of compression applied at mid descending phase. ***p<0.001 vs. control. (**F**) Recordings of PER2::Luc IVDs subjected to compression (0.5 MPa, 1 Hz, 1 hr). Each trace is the mean of 3 explants. (**G**) Expression of *Bmal1* and *Cry1* in a rat IVD NP cell line following 3 cycles of oppositely phased compression (12 hr at 0.5 MPa /12 hr at 0 MPa). Mean ±SD of 3 cultures.

Hyperosmolarity (but not hypo-osmolarity) phenocopies the effect of mechanical loading

The diurnal pattern of mechanical loading of the articular cartilage and IVDs is associated with daily changes in osmotic pressure. Under load, the pressurized interstitial fluid flows to regions of lower pressure, resulting in increased osmolarity. When unloaded the process is reversed, causing reduced osmolarity. These changes in osmolarity play an important role in normal skeletal physiology by promoting synthesis of the extracellular matrix (ECM) and stabilising

cellular phenotypes (*20-22*). Therefore, we tested how circadian rhythms in skeletal tissues operate under different baseline osmolarity conditions or when subjected to acute osmotic challenges. PER2::Luc IVD explants were cultured under static osmotic conditions of 230-730 mOsm for 3 days before synchronisation and recording. Here, despite the wide range of osmotic conditions, the intrinsic circadian pacemaking mechanism was still intact with equivalent circadian amplitude and phase, highlighting the ability of these skeletal tissues to adapt to static changes in their environmental osmolarity (Fig.2A). The periodicity was maintained at close to 24 hours despite drastic differences in baseline osmolarity, indicating that circadian period in these skeletal tissues is "osmolarity-compensated" (Fig.2A).

Next, we analysed how an acute change in osmolarity (as experienced by skeletal tissues on a daily basis) impacts on skeletal clocks. Cartilage tissue explants were placed in iso-osmotic (330 mOsm) or hyperosmotic (530 mOsm) media and allowed to adapt for 3 days before synchronisation and recording. When clocks gradually become desynchronised, the conditioned media were swapped between iso and hyper-adapted explants. The clocks in explants that experienced an increase in osmolarity were resynchronised, with the amplitude recovered to the level at the beginning of the experiment, and robust circadian rhythm continued for the next 4 days. In contrast, explants experiencing a decrease in osmolarity showed gradual loss of rhythmicity, similar to the iso-control explants (Fig.2B). After 4 days the media were swapped back between explants and again the tissues experiencing an increase in osmolarity were resynchronised (Fig. 2B). Clocks in IVD explants showed a very similar response to cartilage, with resynchronisation by increased osmolarity (Fig. 2C and Movie S1).

If altered osmolarity is a key mechanism through which mechanical loading acts on the skeletal clock, it should exert very similar phase and dose dependent effects to mechanical loading. Indeed, a hyperosmotic challenge elicited a very similar direction of phase shifts in a circadian phase-dependent manner comparable to loading (Fig. 2D). The phase response curve (PRC) and the phase transition curve (PTC) demonstrated a type 1 resetting (typical response to a relatively mild physiological clock stimulus) (Fig. S3). The hyperosmolarity induced clock-synchronising effect appears much stronger than loading with improved circadian amplitude at all timepoints except at the trough (Fig. 2E). Similar to loading, the circadian clock response to osmolarity is also "dose" dependent, with a phase delay of up to 9.5 hours (at mid-descending phase) for the +400 mOsm increase (Fig. 2F). Maximal amplitude induction was observed with +300 mOsm

condition (Fig. 2F). The dose dependent clock resetting by both mechanical loading and osmolarity was also observed in cartilage and IVD explants from a different clock gene reporter *Cry1*-Luc mouse (*23*) (Fig. S4).

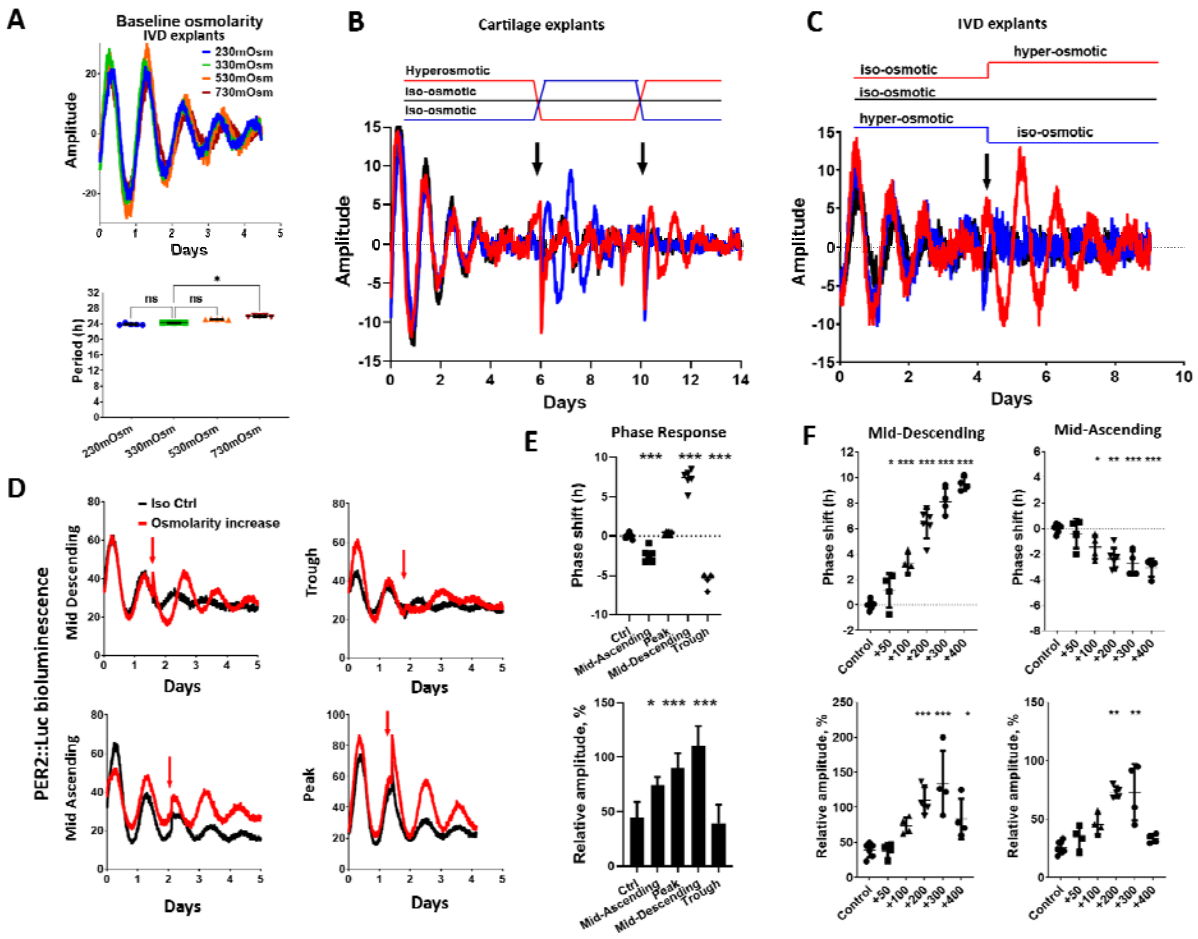

Figure 2. Hyperosmolarity resets the circadian clock in IVDs and cartilage in a phase and dose dependent manner. (**A**) Bioluminescence and period quantification of PER2::Luc IVD explants cultured in varying baseline osmotic conditions. Mean ±SD, n=5. One-way ANOVA (non-parametric Kruskal-Wallis test). *p<0.05; ns, not significant. (**B**) Conditioned media of PER2::Luc cartilage cultured in iso- and hyper- osmotic conditions were switched at day 6, then switched back again at day 10. Control cultures were undisturbed. (**C**) PER2::Luc IVD explants cultured in iso- and hyper- osmotic conditions with media swap at day 4. (**D**) Effects of hyperosmolarity on PER2::Luc IVD oscillations. Explants were subjected to a +200 mOsm increase in osmolarity (red arrow) at 6 hr intervals, starting at 36 hr. (**E**) Quantification of phase shift and amplitude induction in D**.** (**F**) Quantification of dose-dependent phase shift and amplitude induction in PER2::Luc IVD explants treated with increasing osmolarity (+50 to +400 mOsm) at mid descending and mid ascending phase of PER2::Luc oscillation. One-way ANOVA. *p<0.05; **p<0.01; ***p<0.001. For panels A-D, each trace represents mean of 3-6 explants.

Daily hyperosmotic challenge synchronises dampened circadian rhythms in both young and ageing skeletal tissues

With the onset of the activity phase mouse cartilage and IVD tissues experience roughly 12 hours of loading within a 24-hour day, leading to increased osmolarity (*17*). Having determined that the acute increase in osmolarity is a clock synchronising factor, we next used a protocol to approximate the diurnal osmotic cycles experienced by skeletal tissues by exposing cartilage and IVD explants to 12 hours hyperosmotic condition and returning them to 12 hours of iso-osmotic medium. A single cycle with a hyperosmotic challenge as low as +100 mOsm synchronised the circadian rhythm in cartilage (Fig. 3A) and IVDs (Fig. 3B) from young mice (2 months old), although, this effect was clearly dependent on the extent of osmotic change and number of cycles applied. When explants were exposed to two daily cycles of +200 mOsm challenges, they showed an even stronger clock amplitude (Fig. 3C, D). In contrast, exposure of tissue explants to a 1 hr hyperosmotic pulse had no significant effect on phase or amplitude (Fig. S5).

We have previously shown that the circadian amplitude of IVD and cartilage rhythms dampen with ageing (*13*, *15*). Therefore, we tested whether clocks in ageing skeletal tissues still respond to osmotic cycles. Indeed, exposure of ageing explants to two osmotic cycles resulted in resynchronisation of both articular cartilage (Fig. 3E) and in IVDs (Fig. 3F).

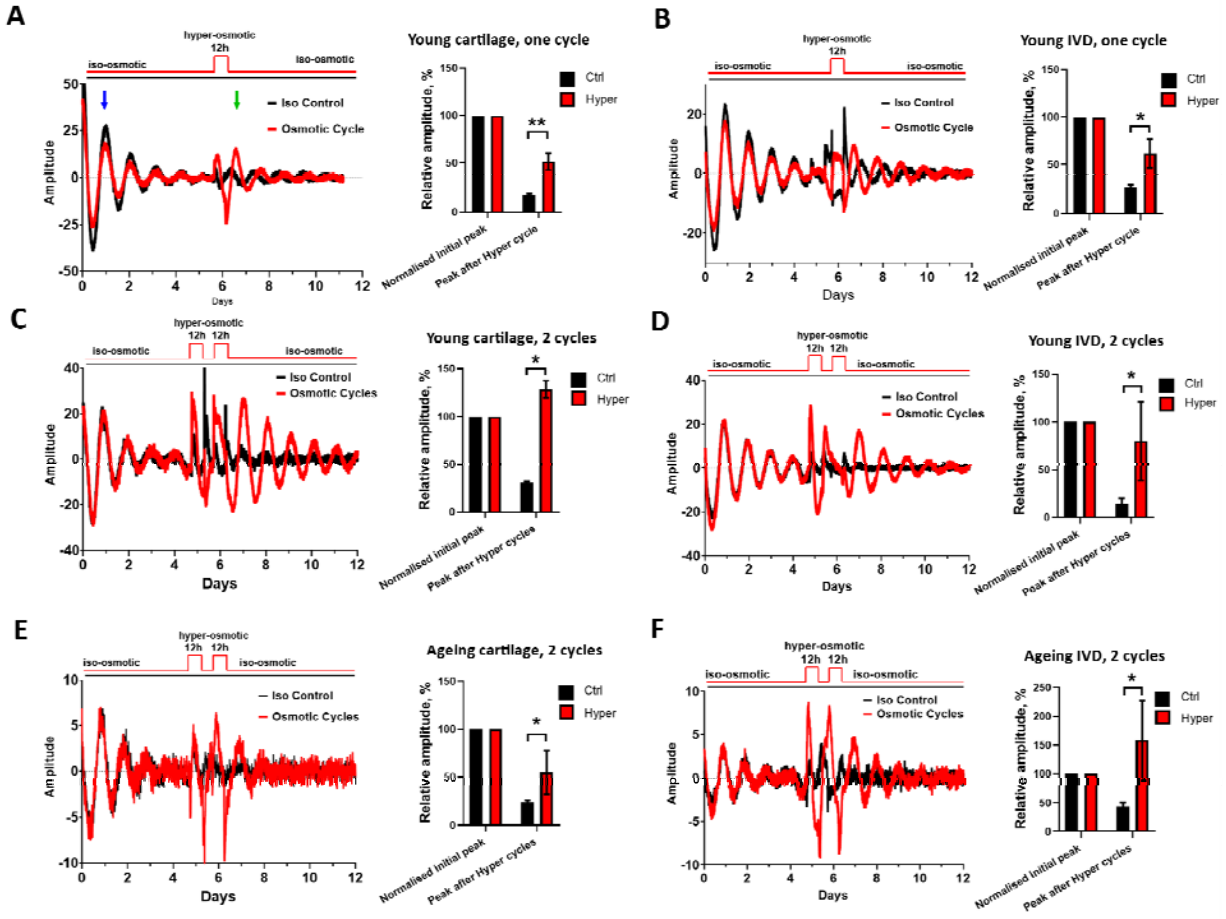

Figure 3. Osmotic cycles synchronise circadian clocks in young and ageing cartilage and IVDs. (**A, B**) Effects of one cycle of osmotic changes on PER2::Luc cartilage explants (A) and IVDs (B) from 2-month old mice. At day 6 explants were exposed to 12 hr of +100 mOsm hyperosmotic medium then returned to iso-osmotic media. Amplitude of the peak after osmotic cycle (green arrow) was quantified as % of the peak 24 hr after start of recording (blue arrow). (**C-F**) Effects of two cycles of hyperosmotic challenges (12 hr of +200 mOsm/12 hr of iso-osmotic media) on cartilage (C, E) and IVDs (D, F) from 2-month old (C and D) or 12-month old (E and F) PER2::Luc mice. Unpaired t-test, *p<0.05; **p<0.01.

Hyperosmotic challenge induces rhythmic global gene expression patterns in a cell-autonomous manner

Next, we wanted to investigate how cellular circadian clocks in isolated cells respond to hyperosmotic challenge. Clock-unsynchronised primary chondrocytes from PER2::Luc mice exhibit only a low amplitude oscillation. Exposure to +200 mOsm increase in osmolarity augmented PER2::Luc amplitude (Fig. 4A). Similar observations were made in a human NP115 (IVD) cell line (Fig. S6A). Strikingly, the same hyper-osmotic stimuli disrupted circadian oscillation in U2OS cells, a human osteosarcoma cell line widely used as a cellular model of

circadian clocks (Fig. S6B). As such, the osmolarity-entrainment of circadian clock is clearly cell type dependent and indicative of cellular adaptation to their local niche.

We next determined to what extent hyperosmolarity can synchronise circadian rhythms of gene expression at the transcriptome level by circadian time-series RNA sequencing in primary mouse chondrocytes. The PER2::Luc reporter allowed us to track clock rhythms in parallel cultures (Fig. 4A). mRNA samples were collected every 4 hours for 2 full circadian cycles, starting with samples just before the osmotic increase (Time 0h). Principal component analysis of the RNAseq results revealed the circadian time of sampling as the biggest factor separating the samples (Fig. 4B). MetaCycle analysis revealed 1,312 rhythmic genes using integrated P<0.05 cut-off threshold (254 rhythmic genes with a BHQ<0.05 cut-off), including most core clock genes (Fig. 4C, D; Data S1, S2). IPA analysis revealed significantly rhythmic pathways including “Circadian Rhythm Signalling”, “Protein Ubiquitination Pathway”, “mTOR Signalling” and “Autophagy” (Data S3).

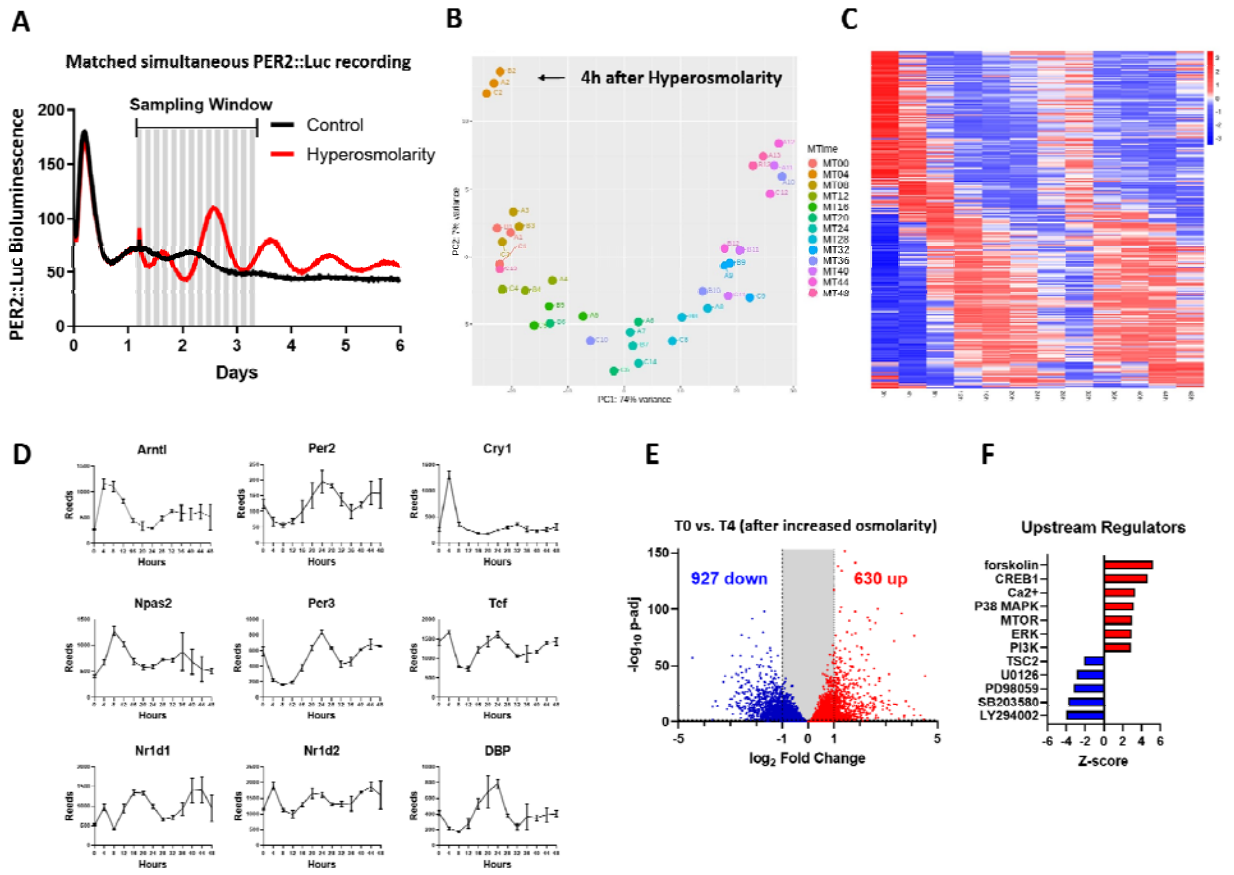

Figure 4. Hyperosmolarity induces wide scale rhythmic gene expression at the transcriptome level. (**A**) Bioluminescence recording of primary chondrocytes isolated from PER2::Luc mice. Cells were not synchronised at the beginning of the experiment. After 30 hr, media osmolarity was increased by +200 mOsm. Parallel samples were harvested every 4 hr for RNA isolation and RNAseq analysis. (**B**) Principal component analysis showing correlation of RNAseq replicates and a developing trend over time. (**C**) Heatmap showing gene expression patterns of 254 rhythmic genes (BHQ<0.05) following increase of osmolarity. (**D**) RNAseq raw data for core circadian clock genes following increase of osmolarity (Mean ±SD, N=3). (**E**) Volcano plot showing differentially expressed genes between T0 and T4 (4 hr after increase in osmolarity). 1,557 genes showed significant changes (>2-fold, p-adj<0.05). (**F**) IPA prediction of top upstream regulators for differentially expressed genes between T0 vs. T4. Red, positive correlation; blue, negative correlation.

Hyperosmolarity- induced clock resetting involves ERK1/2 and p38, but not CREB or Ca^{2+}

To gain mechanistic insights into how hyperosmolarity induced pathways link to the circadian clocks we performed IPA Upstream Regulators analysis based on differential genes (1,557 immediate response genes with >2-fold change) between T0 and T4 (Fig. 4E, Data S4). This analysis showed Forskolin (a known circadian clock synchronising compound) along with CREB1 as the most over-represented activator (P<0.001). Other significant upstream regulators included p38, Ca^{2+}, ERK and mTOR (Fig. 4F, Data S5). Treatment with forskolin had a synchronising effect on IVD clocks (Fig.S7A). However, inhibitors of CREB had no effect on blocking the hyperosmolarity induced rhythms (Fig. S7B, C). Equally, hyperosmolarity (or mechanical loading) elicited similar clock changes in IVD, cartilage and primary chondrocytes regardless of the presence or absence of calcium in the medium, nor the presence of Gd^{3+}, a wide-spectrum cell membrane calcium channel blocker (Fig. S8A-D). Western blotting confirmed activation of ERK1/2 and p38 upon hyperosmotic challenge in mouse primary chondrocytes (Fig.S9A, C), consistent with earlier reports (*24*, *25*). Inhibition of ERK1/2, p38, or MEK (upstream of ERK1/2) blocked the amplitude effect of hyperosmotic challenge in PER2::Luc IVDs (Fig. S9B, D; Fig.S10A, B). However, these inhibitors did not have any significant effect on loading-induced clock resetting (Fig. S11A, B).

mTORC2-AKT-GSK3β as a convergent pathway for loading and hyperosmolarity induced clock resetting

Another pathway that featured prominently both in Upstream Regulators and in KEGG analysis of the upregulated genes by hyperosmolarity was mTOR (Data S5). Therefore, we tested two mTOR inhibitors, Torin1 (blocking both mTORC1 and mTORC2 complex) and Rapamycin

(primarily blocking mTORC1). While Torin1 completely blocked the increase in amplitude following hyperosmotic challenge in cartilage and IVD explants, Rapamycin had no effect (Fig. 5A, B, Fig. S12), indicating involvement of mTORC2. AKT (PKB) is a well-known phosphorylation target of mTORC2 (*26*) and can be activated by hyperosmolarity in renal cells (*27*). Indeed, pre-treatment of tissue explants with an AKT inhibitor prevented the increase in circadian amplitude following hyperosmotic challenge (Fig. 5C). AKT is a known upstream regulator of GSK3β activity, a key clock regulating kinase which has been implicated in the regulation of the stability and/or nuclear translocation of PER2, CRY2, CLOCK, REV-ERBα and BMAL1 (*28-30*). Indeed, hyperosmotic challenge increased GSK3β phosphorylation at Ser9 and Ser389 (corresponding to reduced activity) (Fig. 5D). Concordantly, inhibition of GSK3β activity by lithium had a synchronising effect on IVD clocks similar to that of hyperosmolarity (Fig. 5E). Pre-treatment with Torin1 (but not Rapamycin) or an AKT inhibitor decreased GSK3β phosphorylation at Ser9 and Ser389 following hyperosmotic challenge (Fig. 5F-H). We next tested whether the above mechanisms were also involved in clock resetting by mechanical loading. Pre-treatment with the mTORC2 or AKT inhibitor completely blocked the mechanical loading induced increase in circadian clock amplitude (Fig. 5I, J). However, Rapamycin did not have any significant effect on loading-induced clock resetting (Fig. S11C). Supporting our findings, mechanical strain in mesenchymal stem cells initiates a signalling cascade that is uniquely dependent on mTORC2 activation and phosphorylation of AKT at Ser-473, an effect sufficient to cause inactivation of GSK3β (*31*). The convergent mTORC2-AKT-GSK3β pathway supports osmolarity change as an important downstream factor in mediating loading-entrained skeletal clocks.

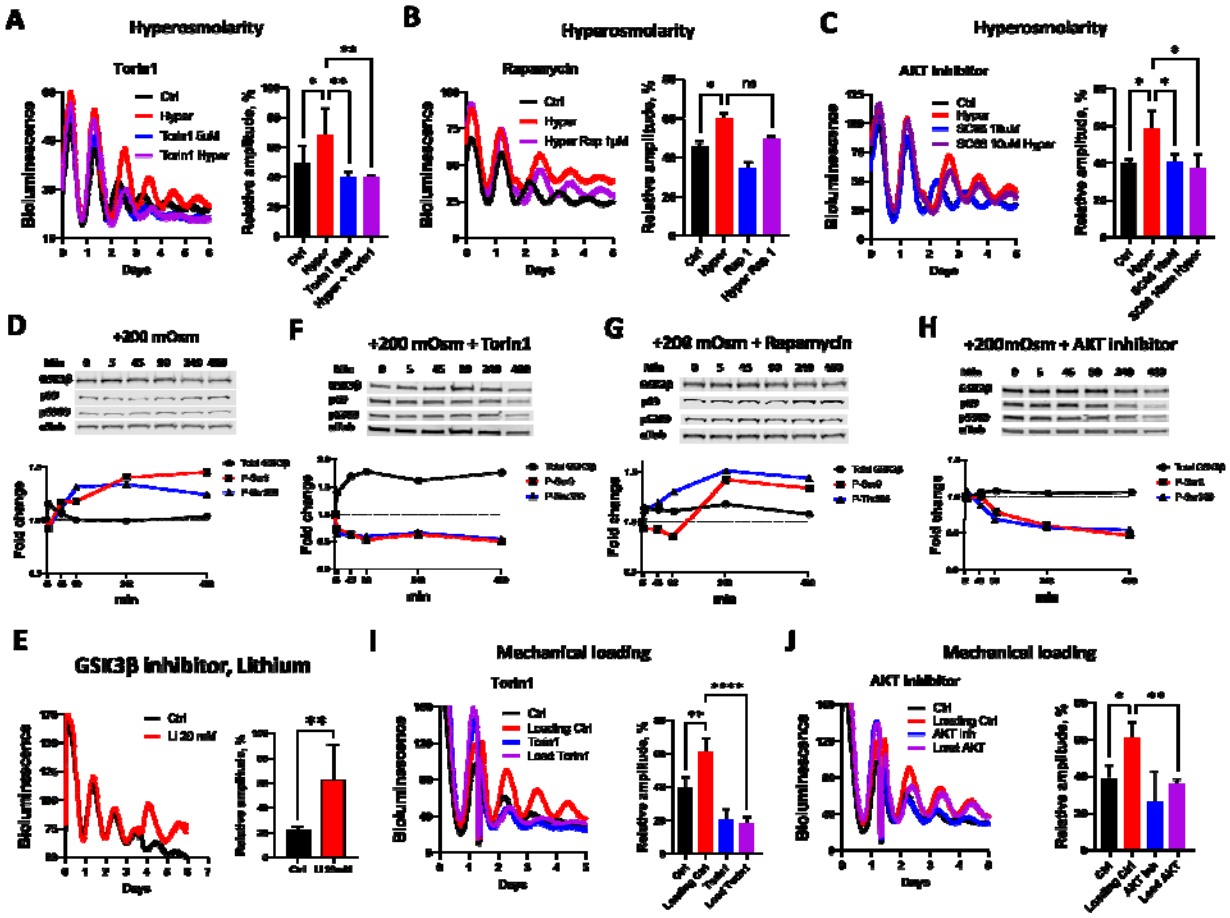

Figure 5. The mTORC2-AKT-GSK3β pathway is a convergence mechanism mediating the loading and hyperosmolarity elicited clock entrainment. (A-C) Effects of mTORC1/2 inhibitor Torin1 (A), mTORC1 inhibitor Rapamycin (B) and AKT inhibitor SC66 (C) on blocking the hyperosmolarity (+200 mOsm) -induced clock amplitude in PER2::Luc cartilage explants. **(D)** WB showing total and phosphorylation levels of GSK3β at Ser9 and Ser389 in response to +200 mOsm change in osmolarity in mouse primary chondrocytes. **(E)** Bioluminescence recording and amplitude quantification of PER2::Luc IVD explants treated with 20 mM lithium (an inhibitor of GSK3β). **(F-H)** Effects of Torin1 (F), Rapamycin (G) and AKT inhibitor SC66 (H) on blocking the hyperosmolarity-induced phosphorylation of GSK3β at Ser9 and Ser379 in mouse primary chondrocytes. **(I, J)** Effects of Torin1 (I) or the AKT inhibitor SC66 (J) on blocking the loading (0.5 MPa, 1 Hz, 1 hr) induced clock amplitude change in PER2::Luc cartilage explants. Unpaired t-test for E. **p<0.01. One-way ANOVA for A, B, C, I and J. *p<0.05; **p<0.01; ****p<0.0001; ns- not significant.

Taken together, we have identified daily cycles of mechanical loading and associated rhythmic changes of osmolarity within the physiological range as bona fide entrainment cues for skeletal circadian clocks. These time cues are particularly important for tissues such as the IVD and cartilage because they are isolated from vascular, lymphatic and nervous systems, yet their circadian rhythms are sensitive to age-related dampening (*12*). We show that repeated daily

osmotic cycles lead to resynchronisation of circadian rhythm in ageing tissue explants, supporting a hypothesis that reduced rest/activity patterns in ageing individuals could contribute to skeletal clock disruptions *in vivo*.

The clock resetting effect by loading and hyperosmolarity is circadian phase dependent. An osmotic increase or loading at the peak of PER2::Luc (which corresponds to the activity onset in mice) does not shift the phase but strengthens the amplitude of skeletal clocks, which could have implications for the timing of exercise. Incidentally, early morning was shown as the most beneficial time to engage in aerobic exercise in humans to enhance nocturnal blood pressure "dips" and improve quality of sleep (*32*). Regular low- to medium-intensity exercise is thought to be beneficial for the maintenance of skeletal muscle, joint and IVD (*33, 34*). Indeed, scheduled exercise was shown to reset the circadian clocks in a time-dependent manner in the SCN, skeletal muscle and adrenal gland (*35-38*). However, these studies have largely focused on metabolic and stress related pathways downstream of exercise, instead of the role of mechanical loading or osmolarity.

We show that skeletal clock period is osmolarity-compensated and clock phase shows a type 1 resetting (relatively mild, similar to the SCN's response to light). A study reported a 30 min hypertonic pulse of +600 mOsm led to clock phase shifts and a type 0 resetting in MEFs, NIH3T3 and U2OS cells (*39*). However, +600 mOsm is well outside the physiological range of most human or mouse cells. In the nucleus pulposus region of IVD where extracellular osmolarity is the greatest, osmolarity fluctuates between 400 to 550 mOsm while in cartilage it varies between 350 and 480 mOsm (*17*), depending on the time of day. Indeed, we found chronic +200 mOsm was well tolerated by skeletal cells but showed a severe detrimental effect on clocks in U2OS cells. As such, the clock entrainment effect by physiological fluctuations of osmolarity is clearly specific to the unique skeletal tissue niche.

Based on our findings, it is plausible to predict that daily surges of osmolarity, at the starting phase of activity, may serve as a critical mechanism for skeletal tissues to sense the passage of time and keep its endogenous rhythm in sync with the external environment. As such, our findings resolve the question of how the cartilage and IVD clocks are entrained and confirm tissue-unique inputs as a feature of circadian organisation in mammals. These physiological inputs may allow flexibility for cartilage/IVD clocks to be uncoupled from the SCN clock when required. Indeed, when typical nocturnal animals are energetically challenged by food shortage

or thermal stress, they switch temporal niche from nocturnal to diurnal (*40-41*). These biological insights will also help us understand how ageing and a sedentary lifestyle impact on circadian rhythms and facilitate design of time-prescribed interventions to maintain musculoskeletal health.

References

1. Reppert SM, Weaver DR. Coordination of circadian timing in mammals. Nature. 2002;418(6901):935-41.

2. Takahashi JS. Transcriptional architecture of the mammalian circadian clock. Nat Rev Genet. 2017;18(3):164-79.

3. Hastings MH, Reddy AB, Maywood ES. A clockwork web: circadian timing in brain and periphery, in health and disease. Nat Rev Neurosci. 2003;4(8):649-61.

4. Cederroth CR, et al. Medicine in the fourth dimension. Cell metabolism. 2019;30(2):238-50.

5. Zeng H, Qian Z, Myers MP, Rosbash M. A light-entrainment mechanism for the Drosophila circadian clock. Nature. 1996;380(6570):129-35.

6. Balsalobre A, Brown SA, Marcacci L, Tronche F, Kellendonk C, Reichardt HM, et al. Resetting of circadian time in peripheral tissues by glucocorticoid signaling. Science. 2000;289(5488):2344-7.

7. Brown SA, Zumbrunn G, Fleury-Olela F, Preitner N, Schibler U. Rhythms of mammalian body temperature can sustain peripheral circadian clocks. Current biology. 2002;12(18):1574-83.

8. Buhr ED, Yoo SH, Takahashi JS. Temperature as a universal resetting cue for mammalian circadian oscillators. Science. 2010;330(6002):379-85.

9. Damiola F, Le Minh N, Preitner N, Kornmann B, Fleury-Olela F, Schibler U.et al. Restricted feeding uncouples circadian oscillators in peripheral tissues from the central pacemaker in the suprachiasmatic nucleus. Genes Dev. 2000;14(23):2950-61.

10. Stokkan KA, Yamazaki S, Tei H, Sakaki Y, Menaker M. Entrainment of the circadian clock in the liver by feeding. Science. 2001;291(5503):490-3.

11. Crosby P, et al. Insulin/IGF-1 drives PERIOD synthesis to entrain circadian rhythms with feeding time. Cell. 2019;177(4):896-909.

12. Morris H, Goncalves CF, Dudek M, Hoyland J, Meng QJ. Tissue physiology revolving around the clock: circadian rhythms as exemplified by the intervertebral disc. Annals Rheum Dis. 2021; 80:828-839.

13. Gossan N, et al. The circadian clock in murine chondrocytes regulates genes controlling key aspects of cartilage homeostasis. Arthritis and rheumatism. 2013;65(9):2334-45.

14. Dudek M, et al. The chondrocyte clock gene Bmal1 controls cartilage homeostasis and integrity. J Clin Invest. 2016;126(1):365-76.

15. Dudek M, et al. The intervertebral disc contains intrinsic circadian clocks that are regulated by age and cytokines and linked to degeneration. Annals Rheum Dis. 2017;76(3):576-84.

16. Akagi R, et al. Dysregulated circadian rhythm pathway in human osteoarthritis: NR1D1 and BMAL1 suppression alters TGF-beta signaling in chondrocytes. Osteo Cartilage. 2017;25(6):943-51.

17. Bekki H, et al. Suppression of circadian clock protein cryptochrome 2 promotes osteoarthritis. Osteoarthritis and cartilage. 2020;28(7):966-76.

18. Gerber A, et al. Blood-borne circadian signal stimulates daily oscillations in actin dynamics and SRF activity. Cell 2013; 152(3): 492-503.

19. Yoo SH, et al. PERIOD2::LUCIFERASE real-time reporting of circadian dynamics reveals persistent circadian oscillations in mouse peripheral tissues. Proc Natl Acad Sci USA. 2004; 101: 5339-5346.

20. Urban JP, Hall AC, Gehl KA. Regulation of matrix synthesis rates by the ionic and osmotic environment of articular chondrocytes. J Cell Physiol. 1993;154(2):262-70.

21. Li P, et al. Osmolarity affects matrix synthesis in the nucleus pulposus associated with the involvement of MAPK pathways: A study of ex vivo disc organ culture system. J Orthop Res. 2016;34(6):1092-100.

22. Palacio-Mancheno PE, Evashwick-Rogler TW, Laudier DM, Purmessur D, Iatridis JC. Hyperosmolarity induces notochordal cell differentiation with aquaporin3 upregulation and reduced N-cadherin expression. J Orthop Res. 2018;36(2):788-98.

23. Maywood ES, et al. Analysis of core circadian feedback loop in suprachiasmatic nucleus of mCry1-luc transgenic reporter mouse. Proc Natl Acad Sci USA. 2013; 110(23): 9547-9552.

24. Tsai TT, et al. MEK/ERK signaling controls osmoregulation of nucleus pulposus cells of the intervertebral disc by transactivation of TonEBP/OREBP. J Bone Miner Res. 2007;22(7):965-74.

25. Li H, Wang J, Li F, Chen G, Chen Q. The influence of hyperosmolarity in the intervertebral disc on the proliferation and chondrogenic differentiation of nucleus pulposus-derived mesenchymal stem cells. Cells Tissues Organs 2018; 205:178-188.

26. Moore SF, Hunter RW, Hers I. mTORC2 protein complex-mediated Akt (Protein Kinase B) Serine 473 Phosphorylation is not required for Akt1 activity in human platelets. J Biol Chem. 2011;286 (28): 24553-60.

27. Terada Y, et al. Hyperosmolality activates Akt and regulates apoptosis in renal tubular cells. Kidney Int. 2001; 60(2): 553-67.

28. Iitaka C, Miyazaki K, Akaike T, Ishida N. A role for glycogen synthase kinase-3beta in the mammalian circadian clock. J Biol Chem. 2005; 280: 29397-29402.

29. Harada Y, Sakai M, Kurabayashi N, Hirota T, Fukada Y. Ser-557-phosphorylated mCRY2 is degraded upon synergistic phosphorylation by glycogen synthase kinase-3 beta. J Biol Chem. 2005; 280: 31714-31721.

30. Yin L, Wang J, Klein PS, Lazar MA. Nuclear receptor Rev-erbalpha is a critical lithium-sensitive component of the circadian clock. Science 2006; 311: 1002-1005.

31. Case N, et al. Mechanical regulation of glycogen synthase kinase 3β (GSK3β) in mesenchymal stem cells is dependent on Akt protein serine 473 phosphorylation via mTORC2 protein. J Biol Chem. 2011; 286 (45): 39450-6.

32. Fairbrother K, et al. Effects of exercise timing on sleep architecture and nocturnal blood pressure in prehypertensives. Vasc Health Risk Manag. 2014; 10: 691-698.

33. Cartee GD, et al. Exercise promotes healthy aging of skeletal muscle. Cell Metabolism 2016;23(6):1034-47.

34. Belavý DL, et al. Running exercise strengthens the intervertebral disc. Sci Rep. 2017;7(1):45975.

35. Schroeder AM, et al. Voluntary scheduled exercise alters diurnal rhythms of behaviour, physiology and gene expression in wild-type and vasoactive intestinal peptide-deficient mice. J Physiol. 2012; 590(23): 6213-26.

36. Wolff G and Esser KA. Scheduled exercise phase shifts the circadian clock in skeletal muscle. Med Sci Sports Exerc. 2012; 44(9):1663-70.

37. Zambon AC, et al. Time- and exercise-dependent gene regulation in human skeletal muscle. Genome Biol. 2003;4(10): R61.

38. Kemler D, Wolff CA, Esser KA. Time of day dependent effects of contractile activity on the phase of the skeletal muscle clock. J Physiol. 2020; 598 (17): 3631-3644.

39. Imamura K, et al. ASK family kinases mediate cellular stress and redox signaling to circadian clock. Proc Natl Acad Sci U S A. 2018; 115(14): 3646-3651.

40. Hut RA, Pilorz V, Boerema AS, Strijkstra AM, Daan S. Working for food shifts nocturnal mouse activity into the day. PLoS ONE. 2011; 6(3): e17527.

41. van der Vinne V, et al. Cold and hunger induce diurnality in a nocturnal mammal. Proc Natl Acad Sci USA. 2014;111(42):15256-60.

Acknowledgments:

We thank M Hastings (MRC LMB, Cambridge, UK) and J Takahashi (UT Southwestern Medical Center, US) for the *Cry1*-Luc and PER2::Luc mouse lines. We thank GC Van Den Akker, TJ Welting and JW Voncken (Maastricht University, Netherlands) for their kind provision of the human NP115 cell line. We thank the Genomics Core Facility (A Hayes and L Zeef) and the Bioimaging Facility (D Spiller) at the University of Manchester for their kind assistance with RNAseq and imaging studies. We thank R Lucas and J Allen for their comments on our manuscript.

Funding:

MRC project grants MR/T016744/1 and MR/P010709/1 (QJM, JAH).

Versus Arthritis Senior Fellowship Award 20875 (QJM).

Wellcome Trust Grant for the Wellcome Centre for Cell-Matrix Research 088785/Z/09 (QJM).

Funds for International Cooperation and Exchange of the National Natural Science Foundation of China, Grant No. 82020108019 (ZJL).

Author contributions:

Conceptualization: QJM, JAH, MD

Methodology: MD, DP, CL, DW, LY

Investigation: MD, DP, CG, DW, CL, LY, ZJL, QJM, JAH

Visualization: MD, CG, CL, DW.

Funding acquisition: QJM, JAH, ZJL

Project administration: QJM, JAH

Supervision: QJM, JAH

Writing – original draft: QJM, MD, JAH

Writing – review & editing: LY, ZJL

Competing interests: Authors declare that they have no competing interests.

Data and materials availability: All data are available in the main text or the supplementary materials.

Supplementary Materials:

Materials and Methods

Figs. S1 to S12

Data S1 to S5

References (1-12)

Movie S1